

See discussions, stats, and author profiles for this publication at: <https://www.researchgate.net/publication/221972382>

# 7-Ethynylcoumarins: Selective Inhibitors of Human Cytochrome P450s 1A1 and 1A2

ARTICLE in CHEMICAL RESEARCH IN TOXICOLOGY · MARCH 2012

Impact Factor: 3.53 · DOI: 10.1021/tx300023p · Source: PubMed

CITATIONS

9

READS

28

8 AUTHORS, INCLUDING:



Jiawang Liu

Xavier University of Louisiana

44 PUBLICATIONS 270 CITATIONS

SEE PROFILE



Jayalakshmi Sridhar

Xavier University of Louisiana

25 PUBLICATIONS 358 CITATIONS

SEE PROFILE



Xiaoyi Zhang

Fudan University

38 PUBLICATIONS 189 CITATIONS

SEE PROFILE



Maryam Foroozesh

Xavier University of Louisiana

52 PUBLICATIONS 726 CITATIONS

SEE PROFILE

Published in final edited form as:

*Chem Res Toxicol.* 2012 May 21; 25(5): 1047–1057. doi:10.1021/tx300023p.

## 7-Ethynylcoumarins: Selective Inhibitors of Human Cytochrome P450s 1A1 and 1A2

Jiawang Liu<sup>†</sup>, Thong T. Nguyen<sup>†</sup>, Patrick S. Dupart<sup>†</sup>, Jayalakshmi Sridhar<sup>†</sup>, Xiaoyi Zhang<sup>†</sup>, Naijue Zhu<sup>†</sup>, Cheryl L. Klein Stevens<sup>§</sup>, and Maryam Foroozesh<sup>†,\*</sup>

<sup>†</sup>Department of Chemistry, Xavier University of Louisiana, New Orleans, Louisiana 70125, United States

<sup>‡</sup>College of Pharmaceutical Sciences, Capital Medical University, Beijing 100069, PR China

### Abstract

To discover new selective mechanism-based P450 inhibitors, eight 7-ethynylcoumarin derivatives were prepared through a facile two-step synthetic route. Cytochrome P450 activity assays indicated that introduction of functional groups in the backbone of coumarin could enhance the inhibition activities toward P450s 1A1 and 1A2, providing good selectivity against P450s 2A6 and 2B1. The most potent product 7-ethynyl-3,4,8-trimethylcoumarin (7ETMC) showed IC<sub>50</sub> values of 0.46  $\mu$ M and 0.50  $\mu$ M for P450s 1A1 and 1A2 in the first six minutes, respectively, and did not show any inhibition activity for P450s 2A6 and 2B1 even at the dose of 50  $\mu$ M. All of the inhibitors except 7-ethynyl-3-methyl-4-phenylcoumarin (7E3M4PC) showed mechanism-based inhibition of P450s 1A1 and 1A2. In order to explain this mechanistic difference in inhibitory activities, X-ray crystallography data were used to study the difference in conformation between 7E3M4PC and the other compounds studied. Docking simulations indicated that the binding orientations and affinities resulted in different behaviors of the inhibitors on P450 1A2. Specifically, 7E3M4PC with its two-plane structure fits into the P450 1A2's active site cavity with an orientation leading to no reactive binding, causing it to act as a competitive inhibitor.

### Introduction

Cytochrome P450 enzymes are a large superfamily of hemoprotein monooxygenases involved in the metabolism, detoxification, and bioactivation of endogenous and xenobiotic chemicals and also associated with the formation and development of certain cancers.<sup>1,2</sup> Therefore, developing selective P450 enzyme inhibitors has attracted considerable attention over the years.<sup>3,4</sup> P450s 1A1 and 1A2 play important roles in the bioactivation of a variety of procarcinogenic polycyclic aromatic hydrocarbons.<sup>5,6</sup> As a classic example, benzo[*a*]pyrene could be metabolized by P450s 1A1 and 1A2 into benzo[*a*]pyrene-7,8-diol-9,10-epoxide, the ultimate mutagen, which could form DNA and protein adducts, leading to tumor formation and organ toxicity.<sup>6,7</sup> Another example is that of the bioactivation of aflatoxin B1 mainly by P450s 1A2, 2B1, and 3A4 to form a reactive epoxide intermediate, acting as a DNA intercalating and alkylating agent and resulting in an increased risk of cancer formation.<sup>8-10</sup> In addition, recent epidemiological evidence suggest

\*To whom correspondence should be addressed Department of Chemistry Xavier University of Louisiana 1 Drexel Dr. New Orleans, LA 70125 Tel: 504-520-5078 Fax: 504-520-7942 mforooze@xula.edu.

<sup>§</sup>Present address: Ogden College of Science and Engineering, Western Kentucky University, 1906 College Heights Boulevard #11075, Bowling Green, Kentucky 42101-1075, United States

**Supporting information** The Crystallographic Information File (cif) was supplied in the Supporting Information I. The raw <sup>13</sup>C NMR spectra, raw elemental analysis reports, and HPLC purity reports were contained in Supporting Information II.

that genetic polymorphisms of human *CYP1A1* and *1A2* genes show significant correlation with the susceptibilities to lung and breast cancers.<sup>11-13</sup> Therefore, it is expected that inhibitors of P450s 1A1 and 1A2 could be developed to serve as cancer chemo-preventive agents, especially for individuals exposed to polycyclic aromatic hydrocarbon procarcinogens due to their occupation or high-level environmental pollution.<sup>14-16</sup>

A number of small molecules including polycyclic aromatic hydrocarbons, coumarins, flavones, and anthraquinones have been developed in our laboratory and evaluated for their inhibition of various P450 enzymes.<sup>17-21</sup> Among these planar molecules, coumarins are known substrates for a number of P450 enzymes (such as P450s 1A1, 1A2, 3A4, 2A6 and P450s from the 2B subfamily). P450 2A6 metabolizes coumarin into 7-hydroxycoumarin through a 7-hydroxylation reaction, which accounts for more than 70% of the coumarin metabolism in humans. Both 7-ethoxycoumarin and 7-ethoxy-4-(trifluoromethyl)coumarin are known substrates for the P450 2B enzymes, and their major metabolites are also 7-hydroxycoumarins.<sup>22-23</sup> Coumarin could also be metabolized by P450s 1A1, 1A2, and 3A4 into coumarin-3,4-epoxide and 3-hydroxycoumarin through minor pathways.<sup>24</sup> Thus, coumarin derivatives are expected to be potential substrates and/or inhibitors for P450 enzymes.

In this study, in order to develop a group of coumarin derivatives which selectively inhibit P450s 1A1 and 1A2 but are not metabolized by P450 2A6 and those from the 2B subfamily, the key metabolic site (7-position) on coumarin was modified (Figure 1). Since a number of aromatic acetylenic molecules have been shown to inactivate P450s in a mechanism-based manner, and their metabolic site has been shown to be the acetylene group, the acetylene functional group was chosen to modify the 7-position of coumarin (Figure 1).<sup>25-28</sup> The design of these 7-ethynylcoumarins was thus expected to yield selective mechanism-based inhibitors of P450s 1A1 and 1A2.

Starting from substituted 7-hydroxycoumarins, eight 7-ethynylcoumarins were synthesized through a facile two-step reaction route. The products were evaluated as potential inhibitors of P450s 1A1, 1A2, 2A6, and 2B1 in order to identify the extent of the inhibition activity, dynamic behavior, and selectivity. The  $K_i$  and limiting  $K_{inact}$  values of the mechanism-based inhibitors were determined. Structure-inhibition activity relationships of the 7-ethynylcoumarin derivatives on P450 1A2 were investigated based on the 3D structures of the inhibitors and docking simulations.

## Materials and Methods

### Chemistry

All of the chemicals were purchased from Sigma-Aldrich Corporation (St. Louis, MO) and Fisher Scientific International, Inc. (Hampton, NH). RP-HPLC was performed on an *hp* Hewlett Packard Series 1050 (Column: phenomenex Gemini-NX 5u C18 110A). Mass spectral data were determined by Agilent 6890 GC with a 5973 MS. <sup>1</sup>H NMR and <sup>13</sup>C NMR spectra were recorded on a Varian 300 MHz NMR spectrometer. Elemental analysis was performed by Atlantic Microlab, Inc. (Norcross, GA). X-ray crystal diffraction patterns of 7E3M4PC were recorded on a Bruker AXS SMART<sup>TM</sup> X2S.

### Preparation of 7-Ethynylcoumarin (7EC) (Method A, Scheme 1)

To a solution of 500 mg (3.1 mmol) of 7-hydroxycoumarin in 10 mL of anhydrous pyridine, 1.0 mL (5.9 mmol) of triflic anhydride was added while cooling in an ice bath and under nitrogen atmosphere. The reaction solution was stirred on ice for 2 h before moving into a heating mantle. To this reaction solution, 400 mg (0.57 mmol) of bis(triphenylphosphine)palladium(II) dichloride (Pd(PPh<sub>3</sub>)<sub>2</sub>Cl<sub>2</sub>), 60 mg (0.32 mmol) of CuI,

and 50 mL of diisopropylamine (DIPA) were added. After 10 min of stirring, 800 CL (5.7 mmol) of trimethylsilylacetylene was also added, and the reaction mixture was refluxed for 2 h. It was then allowed to cool to room temperature before quenching with 100 mL of diethyl ether. A black precipitate formed. After filtration, the filtrate was washed with 5% KHSO<sub>4</sub> (50 mL × 7) followed by saturated NaCl (20 mL × 2), dried over anhydrous sodium sulfate, and concentrated under vacuum. The crude 7-trimethylsilylethynylcoumarin intermediate (compound **1**, Scheme 1) was purified through a column chromatography with petroleum ether/ethyl acetate 20:1 as solvent to give 480 mg (Yield, 64%) of a pure grey powder. GC/MS: 242 (M<sup>+</sup>, 20%), 277 ([M-CH<sub>3</sub>]<sup>+</sup>, 100%). <sup>1</sup>H-NMR(CDCl<sub>3</sub>, 300 HMz): δ = 7.588 (d, J = 9.6 Hz, 1H), 7.306~7.109 (m, 3H), 6.334 (d, J = 9.6 Hz, 1H), 0.200 (s, 9H). To a solution of 300 mg (1.2 mmol) of this 7-trimethylsilylethynylcoumarin intermediate in 50 mL of methanol, 1.0 mL (1 M) of tetrabutylammonium fluoride was added. The reaction mixture was stirred at 70 °C for 0.5 h, and quenched with 50 mL of deionized water to form a white precipitate. After filtration, 180 mg (Yield 88%) of the final product was obtained in grey powder form. mp 126-128 °C. GC/MS: 170 (M<sup>+</sup>, 100%), 142 (100), 114 (30), 88 (25), 63 (30). <sup>1</sup>H-NMR(CDCl<sub>3</sub>, 300 HMz): δ = 7.684 (d, J = 9.6 Hz, 1H), 7.447~7.421 (m, 2H), 7.368 (dd, J = 6.8 Hz, J = 1.5 Hz, 1H), 6.433 (d, J = 9.6 Hz, 1H), 3.269 (s, 1H); <sup>13</sup>C-NMR(CDCl<sub>3</sub>, 75 HMz): 142.787, 128.257, 127.923, 120.513, 117.522, 80.808. Anal. Calcd for C<sub>11</sub>H<sub>6</sub>O<sub>2</sub>: C, 77.64; H, 3.55; O, 18.80. Found: C, 76.93; H, 3.52; O, 18.21.

### 7-Ethynyl-6-methoxycoumarin (7E6MOC)

Starting from 7-hydroxy-6-methoxycoumarin, the target compound was prepared by Method A. The colorless crystals were recrystallized from methanol. Yield, 70%. mp 138-141 °C. GC/MS: 200 (M<sup>+</sup>, 100%), 185 (35), 171 (15), 157 (20), 129 (20), 101 (22), 75 (15), 51 (20). <sup>1</sup>H-NMR (CDCl<sub>3</sub>, 300 MHz) δ = 7.635 (d, J = 9.5 Hz, 1H), 7.411 (s, 1H), 6.875 (s, 1H), 6.427 (d, J = 9.5 Hz, 1H), 3.933 (s, 3H), 3.468 (s, 1H). <sup>13</sup>C-NMR (CDCl<sub>3</sub>, 75 MHz) δ = 142.666, 122.229, 117.917, 108.230, 84.756, 56.667. Anal. Calcd for C<sub>12</sub>H<sub>8</sub>O<sub>3</sub>: C, 72.00; H, 4.03; O, 23.98. Found: C, 71.67; H, 4.12; O, 23.59.

### Preparation of 7-Ethynyl-4-methylcoumarin (7E4MC) (Method B, Scheme 1)

To a solution of 500 mg (3.1 mmol) of 7-hydroxycoumarin in 10 mL of anhydrous pyridine, 1.0 mL (5.9 mmol) of triflic anhydride was added while cooling in an ice bath and under nitrogen atmosphere. The reaction mixture was stirred on ice for 2 h before placing in a heating mantle. To this reaction solution, 400 mg (0.57 mmol) of Pd(PPh<sub>3</sub>)<sub>2</sub>Cl<sub>2</sub>, 60 mg (0.32 mmol) of CuI, and 50 mL of diisopropylamine (DIPA) were added. After 10 min of stirring, 800 CL (5.7 mmol) of trimethylsilylacetylene was also added, and the reaction mixture was refluxed for 2 h. The reaction mixture was then concentrated under vacuum to 10 mL before the addition of 1.0 mL (1.0 M) of tetrabutylammonium fluoride in 50 mL of methanol. The reaction mixture was stirred at 70°C for 0.5 h, and then concentrated under vacuum. The residue was purified through a column chromatography with petroleum ether/ethyl acetate 4:1 as solvent to give 260 mg (Yield 50%) of the final product as a grey powder. mp 133-135 °C. GC/MS: 184 (M<sup>+</sup>, 100%), 156 (95), 127 (20), 102 (10), 77 (8), 63 (12), 51 (10). <sup>1</sup>H-NMR (CDCl<sub>3</sub>, 300 HMz) δ = 7.526~7.195 (m, 3H), 6.222 (s, 1H), 3.186 (s, 1H), 2.361 (s, 3H). <sup>13</sup>C-NMR (CDCl<sub>3</sub>, 75 MHz) δ = 128.029, 124.749, 120.619, 115.897, 80.657, 18.723. Anal. Calcd for C<sub>12</sub>H<sub>8</sub>O<sub>2</sub>: C, 78.25; H, 4.38; O, 17.37. Found: C, 77.42; H, 4.47; O, 17.22.

### 7-Ethynyl-3,4,8-trimethylcoumarin (7ETMC)

Starting from 7-hydroxy-3,4,8-trimethylcoumarin, the target compound was prepared by Method A. The colorless crystals were recrystallized from methanol. Yield, 68%. mp 196-198 °C. GC/MS: 212 (M<sup>+</sup>, 100%), 184 (65), 169 (55), 115 (20). <sup>1</sup>H-NMR (CDCl<sub>3</sub>, 300

HMz)  $\delta$  = 7.357 (s, 2H), 3.409 (s, 1H), 2.552 (s, 3H), 2.377 (s, 3H), 2.218 (s, 3H).  $^{13}\text{C}$ -NMR ( $\text{CDCl}_3$ , 75 MHz)  $\delta$  = 127.801, 121.591, 83.481, 81.780, 15.353, 13.743. Anal. Calcd for  $\text{C}_{14}\text{H}_{12}\text{O}_2$ : C, 79.22; H, 5.70. Found: C, 79.29; H, 5.67.

#### 7-Ethynyl-4-(trifluoromethyl)coumarin (7E4TFC)

Starting from 7-hydroxy-4-(trifluoromethyl)coumarin, the target compound was prepared by Method B. Yield, 45 %. mp 147-149 °C. GC/MS: 238 ( $\text{M}^+$ , 100%), 210 (98), 191 (10), 162 (8), 132 (12), 113 (9), 87 (6), 63 (11).  $^1\text{H}$ -NMR ( $\text{CDCl}_3$ , 300 MHz)  $\delta$  = 7.666 (dd,  $J$  = 8.1 Hz,  $J$  = 1.8 Hz, 1H), 7.483 (d,  $J$  = 1.5 Hz, 1H), 7.433 (dd,  $J$  = 8.1 Hz,  $J$  = 1.5 Hz, 1H), 6.797 (s, 1H), 3.338 (s, 1H).  $^{13}\text{C}$ -NMR ( $\text{CDCl}_3$ , 75 MHz)  $\delta$  = 128.773, 127.376, 125.493, 123.368, 121.090, 119.708, 116.717, 116.626, 82.160, 81.674. Anal. Calcd for  $\text{C}_{12}\text{H}_5\text{F}_3\text{O}_2$ : C, 60.52; H, 2.12; O, 13.44. Found: C, 59.93; H, 2.45; O, 13.17.

#### 7-Ethynyl-3-phenylcoumarin (7E3PC)

Starting from 7-hydroxy-3-phenylcoumarin, the target compound was prepared by Method A. Yield, 65%. mp 153-155 °C. GC/MS: 246 ( $\text{M}^+$ , 100%), 218 (60), 189 (50), 109 (10), 94 (15).  $^1\text{H}$  NMR ( $\text{CDCl}_3$ , 300 MHz)  $\delta$  = 7.768 (s, 1H), 7.704~7.675 (m, 2H), 7.489~7.363 (m, 6H), 3.283 (s, 1H).  $^{13}\text{C}$ -NMR ( $\text{CDCl}_3$ , 75 MHz)  $\delta$  = 139.204, 129.335, 128.758, 128.393, 128.029, 125.326, 120.255, 120.012, 82.555, 80.900. Anal. Calcd for  $\text{C}_{17}\text{H}_{10}\text{O}_2$ : C, 82.91; H, 4.09. Found: C, 82.36; H, 4.03.

#### 7-Ethynyl-4-methyl-3-phenylcoumarin (7E4M3PC)

Starting from 7-hydroxy-4-methyl-3-phenylcoumarin, the title compound was prepared by Method B. Yield, 35 %. mp 127-129 °C. GC/MS: 260 ( $\text{M}^+$ , 100%), 231 (50), 202 (30), 155 (10), 101 (8).  $^1\text{H}$ -NMR ( $\text{CDCl}_3$ , 300 MHz)  $\delta$  = 7.600~7.147 (m, 8H), 3.197 (s, 1H), 2.224 (s, 3H).  $^{13}\text{C}$ -NMR ( $\text{CDCl}_3$ , 75 MHz)  $\delta$  = 130.170, 128.697, 128.621, 128.150, 125.357, 120.392, 80.641, 16.719. Anal. Calcd for  $\text{C}_{18}\text{H}_{12}\text{O}_2$ : C, 83.06; H, 4.65. Found: C, 82.18; H, 4.48.

#### 7-Ethynyl-3-methyl-4-phenylcoumarin (7E3M4PC)

Starting from 7-hydroxy-3-methyl-4-phenylcoumarin, the target compound was prepared by Method A. The light yellow crystals were recrystallized from methanol/acetone. Yield, 57 %. mp 159-161 °C. GC/MS: 259 ( $[\text{M}-1]^+$ , 100%), 231 (30), 202 (29), 155 (10), 101 (9).  $^1\text{H}$ -NMR ( $\text{CDCl}_3$ , 300 MHz)  $\delta$  = 7.593~7.473 (m, 4H), 7.297~7.190 (m, 3H), 6.965 (d,  $J$  = 8.2, 1H), 3.239 (s, 1H), 2.024 (s, 3H).  $^{13}\text{C}$ -NMR ( $\text{CDCl}_3$ , 75 MHz)  $\delta$  = 129.198, 129.046, 128.530, 127.832, 127.103, 120.164, 80.171, 15.019. Anal. Calcd for  $\text{C}_{18}\text{H}_{12}\text{O}_2$ : C, 83.06; H, 4.65; O, 12.29. Found: C, 83.03; H, 4.56; O, 12.32.

#### X-ray Crystallography (7E3M4PC)

Single crystals were grown by slow evaporation from an acetone/methanol solution. Data were collected at 173(2) K on a Bruker SMART X2S diffractometer with a microfocus sealed Mo target X-ray tube. The structure was solved and refined using the SHELX-97 software package. All hydrogen atoms were calculated and treated as riding on the parent carbon atom. Corrections for absorption, extinction, and Lorentz and polarization effects were applied. Full-matrix least squares refinement was on  $F^2$  against all reflections. Final  $R$  = 0.0396,  $R_w$  = 0.1078, and  $S$  = 1.022 for  $F^2 > 2\sigma(F^2)$ . A Crystallographic Information File (cif) has been deposited as Supplementary Material.

#### Assays

Human P450 enzymes 1A1, 1A2, and 2A6 (Human CYP1A1, 1A2 and 2A6 + reductase, BD Supersomes<sup>TM</sup>), and rat P450 2B1 enzyme (Rat CYP2B1 + reductase + cytochrome b5, BD

Supersomes™) were purchased from B.D. Biosciences Corporation (Woburn, MA). The P450 1A1, 1A2, and 2B1-dependent activities were assayed in resorufin alkyl ether dealkylation assays using resorufin ethyl ether, resorufin methyl ether, and resorufin pentyl ether fluorescent substrates respectively.<sup>29</sup> P450 2A6-dependent 7-hydroxylation of coumarin was used in a similar assay with minor differences as described below for measuring 2A6 activity.<sup>23</sup>

#### **Ethoxyresorufin O-deethylation (EROD), Methoxyresorufin O-demethylation (MROD), Pentoxyresorufin O-depentylation (PROD), and Coumarin 7-hydroxylation assays**

Potassium phosphate buffer (1760  $\mu$ L of a 0.1 M solution, pH 7.6) was placed in a 1.0 cm quartz cuvette, and 10  $\mu$ L of a 1.0 M  $MgCl_2$  solution, 10  $\mu$ L of a 1.0 mM corresponding resorufin or coumarin substrate solution (f.c. 5  $\mu$ M) in dimethyl sulfoxide (DMSO), 10  $\mu$ L of the microsomal P450 protein (f.c. 5 nM), and 10  $\mu$ L of an inhibitor solution in DMSO were added. For the controls, 10  $\mu$ L of pure DMSO was added in place of the inhibitor solution. The reaction was initiated by the addition of 200  $\mu$ L of a NADPH regenerating solution. The regenerating solution was prepared by combining 797  $\mu$ L of a 0.10 M potassium phosphate buffer solution (pH 7.6), 67  $\mu$ L of a 15 mM  $NADP^+$  solution in buffer, 67  $\mu$ L of a 67.5 mM glucose-6-phosphate solution in buffer, and 67  $\mu$ L of a 45 mM  $MgCl_2$  solution, and incubating the mixture for 5 minutes at 37°C before the addition of 3 units of glucose 6-phosphate dehydrogenase/mL and a final 5 minute incubation at 37°C. The final assay volume was 2.0 mL. The production of resorufin anion was monitored by a spectrofluorimeter (OLIS DM 45 Spectrofluorimetry System) at 530 nm excitation and 585 nm emission, with a slit width of 2 nm. The production of 7-hydroxycoumarin was monitored at 338 nm excitation and 458 nm emission, with a slit width of 2 nm. The reactions were performed at 37°C. For each inhibitor, a number of assay runs were performed using varying inhibitor concentrations (ranging from 0.1 to 100  $\mu$ M). At least four concentrations of each inhibitor showing 20-80% inhibition were tested.

#### **Data Analysis<sup>28</sup>**

**IC<sub>50</sub> values**—The initial data obtained from the above assays were a series of reaction progress curves (the time-course of product formation) in the presence of various inhibitor concentrations and in the absence of the inhibitor as the control (Figure 2A). The Microsoft Excel Program was used to fit these data (fluorescence intensity vs. time) in order to obtain the parameters of the best-fit second-order curves ( $y = ax^2 + bx + c$ ). The coefficient b in the above second-order equation represented enzymatic activity (v). Dixon plots were used (by plotting the reciprocals of the enzymatic activity (1/v) vs. inhibitor concentrations [I]) in order to determine IC<sub>50</sub> values (x-intercepts) for the inhibitors. The results based on the first 6-min enzymatic reaction are tabulated in Table 1.

**K<sub>i</sub> and limiting K<sub>inact</sub> values**—The first-order derivatives ( $y = 2ax + b$ ) of the above second-order curves ( $y = ax^2 + bx + c$ ) represented the enzymatic activity over time. The semilog plots of the percent relative activity versus time as shown in Figure 2B demonstrated the loss of enzymatic activity. The linear portions of the semilog plots (Figure 2B) were used to determine  $t_{1/2}$  ( $0.693/K_{inact}$ ) values at various concentrations for the observed time-dependent losses of activity. To obtain K<sub>i</sub> and limiting K<sub>inact</sub> values of 1/ $K_{inact}$  were plotted versus reciprocals of the inhibitor concentration (1/[I]) (Kitz-Wilson plots). The limiting K<sub>inact</sub> values were obtained from the abscissa intercepts of the plots, and the K<sub>i</sub> values were calculated from the ordinate intercepts ( $8/K_i$ ).

**NADPH Dependency Assay**—To confirm mechanism-based inhibition, pre-incubation assays were performed as follows. All assay solution components had the same concentrations as in the previously described assays. For pre-incubation assays in the



presence of NADPH, potassium phosphate buffer (1560  $\mu\text{L}$  of a 0.1 M solution, pH 7.6) was placed in a 1.0 cm quartz cuvette followed by 10  $\mu\text{L}$  of a 1.0 M  $\text{MgCl}_2$  solution, 10  $\mu\text{L}$  of the microsomal P450 protein, 10  $\mu\text{L}$  of an inhibitor solution in DMSO (f.c., the concentration leading to 20% enzymatic activity inhibition), and 200  $\mu\text{L}$  of a NADPH regenerating solution. The assay mixture was incubated for five minutes at 37°C before reaction initiation by the addition of 200  $\mu\text{L}$  of buffer and 10  $\mu\text{L}$  of the corresponding substrate solution. For the pre-incubation assays in the absence of NADPH, potassium phosphate buffer (1760  $\mu\text{L}$  of a 0.1 M solution, pH 7.6) was placed in a 1.0 cm quartz cuvette followed by 10  $\mu\text{L}$  of a 1.0 M  $\text{MgCl}_2$  solution, 10  $\mu\text{L}$  of the microsomal P450 protein, and 10  $\mu\text{L}$  of an inhibitor solution in DMSO (f.c., the concentration leading to 20% enzymatic activity inhibition). The assay mixture was incubated for five minutes at 37°C, before reaction initiation by the addition of 200  $\mu\text{L}$  of the NADPH regenerating solution and 10  $\mu\text{L}$  of the corresponding substrate solution. The final assay volume for both assays was 2.0 mL. The production of P450-dependent reaction products were monitored as described above. The reactions were performed at 37°C.

**Quenching of P450 1A1 Fluorescence with the 7-Ethynylcoumarins**—The Fluorescence quenching spectra of P450 1A1 with the 7-ethynylcoumarins and their binding constants ( $K_a$ ) were obtained using a method previously reported.<sup>30-32</sup> P450 1A1 was diluted in 0.1 M potassium phosphate buffer (pH 7.6) to form 2.0 mL of a 1.0  $\mu\text{M}$  solution (f.c. 5  $\mu\text{M}$ ), and the fluorescence intensity was measured between 300 and 400 nm (excitation wavelength at 295 nm). Binding of the 7-ethynylcoumarins by P450 1A1 was monitored by detecting decreases in fluorescence intensity after the addition of different concentrations of the 7-ethynylcoumarins (ranging from 0.25 – 10  $\mu\text{M}$ ). The binding constant ( $K_a$ ) of each compound was estimated by linear regression analysis (plotting log of relative fluorescence loss vs. log of Inhibitor concentration) employing the equation  $\log(F_0/F - 1) = \log K_a + n \log [I]$  in the Microsoft Excel Program. The Fluorescence quenching assays were performed at 37°C.

**Docking Simulations of the 7-Ethynylcoumarins in Human P450 1A2**—The *in-silico* studies for 7ECs were carried out using the LigandFit module in Accelrys Discovery Studio® (Accelrys, San Diego, CA). The crystal structure of human cytochrome P450 1A2 in complex with  $\alpha$ -naphthoflavone (PDB ID: 2HI4) is available from the Protein Data Bank (PDB).<sup>33</sup> The active site of P450 1A2 was defined as a sphere of radius 5.37 Å surrounding the  $\alpha$ -naphthoflavone molecule. The water molecules were removed, and hydrogen atoms were added to the P450 template under the CHARMM force field.

The structures of the eight ethynylcoumarin molecules used in this study are presented in Table 1. The 3D structures of 7ECs were built using a 3D-sketcher module in Accelrys Discovery Studio. Partial atomic charges were assigned to each atom with the Gasteiger Charge method, and energy minimization of each molecule was performed using the conjugate gradient method with CHARMM force field. The minimization was terminated when the energy gradient convergence criterion of 0.001 kcal/mol/Å was reached. The 3D structure of compound 7E3M4PC was identified using X-ray crystallography, since the single crystal of 7E3M4PC was prepared in order to investigate the binding postures and orientations.

To explore the binding modes of the 3D-structures of the 7-ethynylcoumarins to P450 1A2, the docking program LigandFit of *Accelrys DS* was used to automatically dock the ligands into the active site cavity of the enzyme. In the LigandFit program, the standard flexible docking protocol was performed. As described by Venkatachalam et al,<sup>34</sup> this method employs a cavity detection algorithm for detecting invaginations in the protein as candidate active site regions. A shape comparison filter is combined with a Monte Carlo

conformational search for generating ligand poses consistent with the active site shape. Candidate poses are minimized in the context of the active site using a grid-based method for evaluating protein-ligand interaction energies.<sup>34</sup> In this case, 20 conformers of each ligand were automatically formed, and docked into the defined active site cavity. The prediction of the ranking of ligands corresponding to their activity was done by a Ligand scoring protocol (including LigScore1&2, PLP1&2, PMF, Jain, and Ludi scoring functions).<sup>34-36</sup> RMS deviation was used to evaluate the accuracy of the docking performance, and the value for the native ligand  $\alpha$ -naphthoflavone was 0.26 Å, suggesting that the accuracy of this docking performance in LigandFit was highly satisfactory.<sup>37-39</sup>

## Results

### Synthesis of 7-Ethynylcoumarins

The synthetic route and conditions for the synthesis of the 7-ethynylcoumarin derivatives are described in scheme 1. The 7-position of the starting materials is activated through the formation of triflate intermediates followed by substitution with the trimethylsilyl-protected acetylene. After removing the protecting group (trimethylsilyl group), the final 7-ethynylcoumarin products are obtained. This synthesis is based on a route previously reported.<sup>25</sup> Since all the reactions involved can occur in basic environment, in this project, a successful improvement was made by the combination of the first two steps (Method A) or all the steps in one pot (Method B). The target compounds 7EC, 7E6MOC, 7ETMC, 7E3PC, and 7E3M4PC were produced by Method A with yields of 56870%, while the other target molecules were synthesized through Method B with yields of 30850%. Based on these results, Method A proved to be a facile pathway to prepare these coumarin derivatives.

### Inhibition Activities of 7ECs on P450s 1A1, 1A2, 2A6, and 2B1

The inhibition activities of compounds 7ECs on P450s 1A1, 1A2, 2A6, and 2B18 dependent reactions were tested through standard methods as previously described.<sup>23,29</sup> Table 1 contains the results observed for the inhibition of P450 1A1-dependent deethylation of resorufin ethyl ether, P450 1A2-dependent demethylation of resorufin methyl ether, P450 2B1-dependent depentylation of resorufin pentyl ether, and P450 2A6-dependent coumarin 7-hydroxylation activities.

The obtained data show a high selectivity for the 7-ethynylcoumarin derivatives toward P450s 1A1 and 1A2 compared to P450s 2A6 and 2B1. Almost all of the studied compounds show inhibition of P450s 1A1 and 1A2 and not P450 2A6, suggesting that the selectivity of these coumarin derivatives for P450s 1A1 and 1A2 are achieved as expected by the design of 7-position acetylene-modified coumarins. Only two of the compounds (7E4TFC & 7E3M4PC) inactivate P450 2B1, suggesting that most of the target compounds possess selectivity for P450s 1A1 and 1A2 compared to 2B1.

Considering the inhibition activities of the coumarin derivatives towards P450s 1A1 and 1A2, the most potent compound on both of these enzymes is compound 7ETMC, with the IC<sub>50</sub> values of 0.50  $\mu$ M and 0.46  $\mu$ M, respectively. Further observation indicates that the compounds with a 4-position mono-substitution (7E4MC & 7E4TFC) more effectively inhibit P450 1A2 than P450 1A1 (around 5-fold difference in the IC<sub>50</sub> values). However, the 3-phenyl substituted compound, 7E3PC, is about five times more potent toward P450 1A1 than P450 1A2. This observation indicates that although P450s 1A1 and 1A2 have a very high degree of similarity (about 80% amino acid sequence similarity), it is possible to develop selective inhibitors for each of them through investigating structure characteristics of their active site cavities.



### Identification of the Inhibition Behavior of 7ECs on 1A1, 1A2, and 2B1

To further study the mode of activity of the inhibitors toward P450s 1A1, 1A2, and 2B1, apparent dissociation constants of enzyme-inhibitor complexes ( $K_I$ ) and apparent rate constants for time-dependent loss of P450-dependent activity (limiting  $K_{inact}$ ) were determined based on the same data obtained from the above enzyme activity assays. The  $IC_{50}$  values could well represent the inhibition activity for the inhibitors with competitive behavior (inhibition degree only depending on the inhibitor's concentration). However, the mechanism-based inhibitors show a time-, concentration-, and NADPH-dependent loss of enzymatic activity (Figure 2A, 2B, and 2D). Therefore, the  $K_I$  and limiting  $K_{inact}$  (dynamic parameter) values of the inhibitors were calculated employing Kitz-Wilson plots (Figure 2C) as shown in Tables 2 and 3.

The inhibitors of P450 1A1 studied here show mechanism-based inhibition behavior. In terms of the inhibition activities toward P450 1A1, the  $K_I$  values vary greatly from 0.57  $\mu M$  to 104.03  $\mu M$  (about 200-fold), while the limiting  $K_{inact}$  values show a relatively small variance from 0.21 to 0.37  $min^{-1}$ . This indicates that the activities of 7ECs on P450 1A1 mainly depend on the binding affinity, and 7ECs possess similar reaction rates with the enzyme. Since this affinity seems to be critical for the inhibition of P450 1A1 by these compounds, another affinity constant, the binding constant ( $K_a$ ), is determined through the fluorescence quenching assay of P450 1A1 by the inhibitors as shown in Table 2.

The inhibition behaviors of 7ECs toward P450 1A2 are not the same as those toward P450 1A1. The compound ranking in the second place (based on the  $IC_{50}$  value of 1.68  $\mu M$ ), 7E3M4PC, does not show a time-dependent loss of enzymatic activity based on the obtained data. Thus, this compound is a competitive inhibitor. As to the inhibitors showing mechanism-based inhibition behavior, the limiting  $K$  values greatly vary, ranging from 0.03  $min^{-1}$  to 0.44  $min^{-1}$  inact (>10 fold). This implies that they have different reaction rates with P450 1A2, resulting from their different reaction abilities and/or probabilities. The following docking simulations of 7ECs in P450 1A2 were done as an effort to explain the differences of the inhibition behaviors based on the binding style and orientation.

For P450 2B1, two inhibitors, 7E4TFC and 7E3M4PC, were analyzed. The results show that 7E4TFC is a competitive inhibitor, while 7E3M4PC acts as a mechanism-based inhibitor. The  $K_I$  and limiting  $K_{inact}$  values of 7E3M4PC are 18.45  $\mu M$  and 0.29  $min^{-1}$ , respectively.

### Single Crystal Structure of 7E3M4PC

During the preparation of the 3D-structures of 7ECs, it was found that the 3D-structure of 7E3M4PC was not similar to the others. Due to the steric H-H and H-CH<sub>3</sub> interactions, the 48 phenyl ring of 7E3M4PC could not rotate freely and favored a torsion angle predicted by Accelrys Discovery Studio to be 64.17° between the phenyl ring plane and the coumarin core plane. The X-ray crystal structure of 7E3M4PC was completed in order to clarify the actual torsion angle between the two planes. The 3D-structure of 7E3M4PC is shown in Figure 3A. The torsion angle was determined to be 68.8(2)° for C13-C12-C3-C4. There are no unusual inter- or intramolecular bonds or angles. There is only a slight difference (RMSD=0.27Å) between the crystal structure conformation and the computer-generated conformation, suggesting a good performance of conformation prediction (Figure 3B). Among the eight molecules, 7E3M4PC is the sole competitive inhibitor of P450 1A2 and the sole mechanism-based inhibitor of P450 2B1, suggesting that the two-plane structure is critical for the inhibition abilities and behaviors observed toward these enzymes. Therefore, docking studies were performed based on the crystallographic coordinates of 7E3M4PC and the computer-generated 3D structures of other 7ECs.

## Docking Simulations of 7ECs Based on the Crystal Complex of P450 1A2 with $\alpha$ -Naphthoflavone

Docking studies were performed with LigandFit in the Accelrys DS studio® according to the protocol described in the Materials and Methods Section. The standard ligand,  $\alpha$ -naphthoflavone, underwent the same process as the test compounds 7ECs (in short, structure sketching and energy minimization), and was then re-docked into the active site cavity of P450 1A2 in order to evaluate the accuracy of the docking performance. Figure 4A shows the overlapped structures of X-ray conformation of  $\alpha$ -naphthoflavone and the docked pose. The root-mean-square deviation (RMSD) value is 0.26 Å, suggesting a good docking performance.

The prediction of the ranking of ligands was done by ligand scoring protocol (including LigScore1&2, PLP1&2, PMF, Jain, and Ludi scoring functions) after the docking process. The comprehensive scores of the docking patterns are represented as consensus values (shown in Table 3). A high consensus value indicates a high affinity ligand. The results show that the docking poses of 7E3PC rank in the first place (Score: 5; the most favorable pose displayed in Figure 4B), and the binding poses of 7E4M3PC rank in the second place (Score: 4; the most favorable pose displayed in Figure 4C). Both of these compounds possess a 3-phenyl functional group and own the lowest  $K_i$  values (0.65 and 0.83  $\mu$ M, respectively) in the P450 1A2 inhibition assays. Specifically, 7E3PC and 7E4M3PC share the same docking orientation with the standard ligand  $\alpha$ -naphthoflavone in the active site cavity of P450 1A2, in which 3-phenyl group faces the enzymatic active center heme, while the coumarin rings are embedded in the narrow cavity formed by Phe226, Phe125, and  $\alpha$ -helix I of the enzyme (Figure 4B and 4C). These observations suggest that the double fitness in both the phenyl pocket and the narrow cavity makes them suitable for the binding site of P450 1A2.

On the other hand, the mid-size 7-ethynylcoumarins (7E6MOC, 7E4MC, 7ETMC and 7E4TFC) got relatively lower scores (from 283) in docking energy evaluation. It was also observed that they could be docked into the enzyme binding site with different poses. Figure 4D-F show three representative poses of 7ETMC in the cavity. Unpredicted, the unsubstituted 7-ethynylcoumarin (7EC) got the poorest score of 0. The crystal conformation of 7E3M4PC could also be docked into the active site cavity with a similar orientation as seen for 7E3PC, 7E4M3PC, and standard ligand (with the phenyl group next to the heme, Figures 4G & 4H).

## Discussion

Using a facile synthetic method, eight 7-ethynylcoumarin derivatives were prepared. Method A (two-step method) gave higher yields than both the one-pot method (Method B) and the original three-step method previously described.<sup>25</sup>

The inhibition activities of these 7-ethynylcoumarins on P450s 1A1, 1A2, 2A6 and 2B1-dependent reactions were studied through enzyme activity assays. As expected, most of the compounds selectively inhibit P450s 1A1 and 1A2 rather than P450s 2A6 and 2B1. 7-ECs act as inhibitors toward P450 1A1 in a mechanism-based manner, and the similar dynamic parameter (limiting  $K_{inact}$ ) values indicate that the inhibitors probably share the same inhibition mechanism and have the same enzyme binding pattern.

For P450 1A2, the inhibition behaviors of compounds differ. Compound 7E3M4PC, possessing a phenyl group in position 4, does not show time- and NADPH-dependent inhibition, acting as a competitive inhibitor. The obviously low limiting  $K_{inact}$  values of compounds 7E3PC and 7E4M3PC, which possess a phenyl group in position 3, suggest

weak reactive abilities of 7E3PC and 7E4M3PC with P450 1A2. Interestingly, the unsubstituted compound 7EC also shows a weak reactive ability with P450 1A2. This indicates that the mid-size 7-ethynylcoumarins (7E6MOC, 7E4MC, 7ETMC and 7E4TFC) are prone to react with P450 1A2 compared to their smaller or bigger counterparts.

To investigate why the high-affinity ligands 7E3PC and 7E4M3PC ( $K_I$  values of 0.65 and 0.83  $\mu\text{M}$ , respectively) show low reactivity with P450 1A2, docking simulations were performed with the LigandFit protocol. The active site cavity of P450 1A2 is made of two tightly connected sections. A narrow water inaccessible cavity (Part A) containing Phe-226 on  $\alpha$ -helix F, Phe-125 in the B'-C loop region with  $\pi$ - $\pi$  interactions (on one side), and the peptide backbone of  $\alpha$ -helix I with hydrophobic interactions (on the other side) (Figure 5A). The  $\pi$ - $\pi$  interactions, non-covalent interactions between aromatic rings, are important forces in molecular recognition, and play an important role in controlling the binding locations and orientations of ligands.<sup>40,41</sup> The geometry preferences and energetic forces of these interactions have been widely studied in recent years. Our earlier studies have demonstrated the importance of aromatic interactions in determining the inhibition potency toward P450 1A2.<sup>19,42</sup> In the case of  $\alpha$ -naphthoflavone, the  $\pi$ - $\pi$  interactions between the flavone ring and the phenyl side chains of Phe-226 (parallel displaced) and Phe-125 (T-Shaped) contribute to the binding affinity. The distance between the two sides of the cavity is about 7.1 – 7.3 Å, resulting in the parallel conformation of the ligand's rigid plane with the phenyl plane of Phe-226 to keep good  $\pi$ - $\pi$  interactions and van-der-waals interactions. A polycyclic aromatic molecule could fit into this cavity. The next section of the cavity (Part B) is a hydrophobic semi-spherical pocket, consisting of the heme residue,  $\alpha$ -helix I, Phe-125, Leu-386, Ile-382, Thr-124, Leu-497, and Thr-498 with hydrophobic interactions. Its maximum diameter is about 10.5 Å, and the minimum diameter is about 9.5 Å (detected according to the crystal structure 2HI4).<sup>33</sup> Thus, Part B can accommodate a group with the size of one phenyl ring at the most, but this group once inside could rotate since there is no direction-oriented residue(s) around this pocket (Figure 5A).

In terms of the poses of 7ETMC (the representative of the mid-size 7-ethynylcoumarins) docked into P450 1A2, several energetically favorable binding poses exist (Figure 5B). This means that 7ETMC could make free rotation with similar binding energies if only it is kept parallel with the Part A's plane forming the  $\pi$ - $\pi$  interactions. Thus, 7ETMC always has the probability that its acetylene group can face the heme residue (Figure 5B, top-left) and react with the enzyme's active center. The other mid-size compounds 7E6MOC, 7E4MC, and 7E4TFC, which show similar reaction rate (limiting  $K_{\text{inact}}$ ) and similar docking scores, probably share a similar reaction probability with 7ETMC.

For the 3-phenyl derivatives, 7E3PC and 7E4M3PC, the docking orientation where the 38 phenyl group faces the heme (Figure 5C left) takes an obvious priority over the acetylene-facing-heme orientation (Figure 5C right). Thus, the reaction probabilities of 7E3PC and 7E4M3PC with the enzyme are greatly lower than that of mid-size coumarins, due to the lower probabilities of the reactive conformation (acetylene group facing the heme). In general, the higher the affinity of the phenyl-facing-heme pose with the enzyme, the lower the probability of a reaction between the acetylene group and the enzyme. This observation explains why compound 7E3PC possesses the highest affinity with P450 1A2 ( $K_I$  0.65  $\mu\text{M}$  and docking score 5), while possessing the lowest reactivity with that enzyme (limiting  $K_{\text{inact}}$  0.03  $\text{min}^{-1}$ ). Therefore, the inhibition activity of compound 7E3PC toward P450 1A2 mainly results from competitive inhibition and not from mechanism-based inhibition.

Based on docking simulations, the 4-phenyl derivative 7E3M4PC fits into the enzyme's active site in one orientation only (the phenyl group facing the heme, Figure 5D left). This is due to the fact that if the 4-phenyl ring is clamped in Part A of the enzyme's active site, the

coumarin bicyclic ring could not be contained in Part B of the enzyme's active site (Figure 5D right). Therefore, compound 7E3M4PC does not show a reactive pose (the acetylene group facing the heme), and its inhibition activity towards P450 1A2 is completely competitive.

All of the inhibitors studied here inactivate P450 1A1 in a mechanism-based manner, suggesting that P450 1A1 accommodates a relatively large range of inhibitors of various sizes compared to P450 1A2. Part B of the P450 1A1 active site cavity is expected to be larger than that of P450 1A2. As of present, the crystal structure of P450 1A1 is still unavailable, and docking studies with P450 1A1 were based on the homology models obtained using modeling programs (such as Composer<sup>TM</sup>, Modeller, SWISS-MODEL, etc).<sup>20,31,43-46</sup> Among these homology modeling studies, Yamazaki et al reported that the volume of the active site of P450 1A1 was larger than that of P450 1A2,<sup>44,47</sup> which is consistent with our observations based on the size of their ligands; while the other studies either reported the opposite<sup>19,48</sup> or did not report this parameter.<sup>20,43</sup> Since the homology modeling studies were performed using different modeling programs and there are no criteria for evaluating homology modeling results obtained from various programs, this debate will continue until the 3D crystal structure of P450 1A1 is reported.

## Supplementary Material

Refer to Web version on PubMed Central for supplementary material.

## Acknowledgments

**Funding Support** NIH-MBRS SCORE (grant number S06 GM 08008) for support of the preliminary work done on this project by the Foroozesh research group.

Louisiana Cancer Research Consortium for purchase of software licenses, NIH-RCMI (grant number G12RR026260) for purchase of the SMART X2S diffractometer and support of the Molecular Structure and Modeling Core, and NIH-SCORE (grant number SC1GM084722) for research support for CLS and salary support for JS.

## ABBREVIATIONS

<b>7EC</b>	7-ethynylcoumarin
<b>7E6MOC</b>	7-ethynyl-6-methoxycoumarin
<b>7E4MC</b>	7-ethynyl-4-methylcoumarin
<b>7ETMC</b>	7-ethynyl-3,4,8-trimethylcoumarin
<b>7E4TFC</b>	7-ethynyl-4-(trifluoromethyl)coumarin
<b>7E3PC</b>	7-ethynyl-3-phenylcoumarin
<b>7E4M3PC</b>	7-ethynyl-4-methyl-3-phenylcoumarin
<b>7E3M4PC</b>	7-ethynyl-3-methyl-4-phenylcoumarin
<b>RMSD</b>	root-mean-square-deviation
<b>DIPA</b>	diisopropylamine
<b>Pd(PPh<sub>3</sub>)<sub>2</sub>Cl<sub>2</sub></b>	bis(triphenylphosphine)palladium(II) dichloride

## References

- (1). Guengerich FP. Cytochrome P450: what have we learned and what are the future issues? *Drug Metab. Rev.* 2004; 36:159–197. [PubMed: 15237850]
- (2). Guengerich FP. Common and uncommon cytochrome P450 reactions related to metabolism and chemical toxicity. *Chem. Res. Toxicol.* 2001; 14:611–650. [PubMed: 11409933]
- (3). Baston E, Leroux FR. Inhibitors of steroidal cytochrome p450 enzymes as targets for drug development. *Recent Pat Anticancer Drug Discov.* 2007; 2:31–58. [PubMed: 18221052]
- (4). Chang TK, Chen J, Yang G, Yeung EY. Inhibition of procarcinogen-bioactivating human CYP1A1, CYP1A2 and CYP1B1 enzymes by melatonin. *J. Pineal. Res.* 2010; 48:55–64. [PubMed: 19919601]
- (5). Ma Q, Lu AY. CYP1A induction and human risk assessment: an evolving tale of in vitro and in vivo studies. *Drug Metab. Dispos.* 2007; 35:1009–1016. [PubMed: 17431034]
- (6). Zhou SF, Chan E, Zhou ZW, Xue CC, Lai X, Duan W. Insights into the structure, function, and regulation of human cytochrome P450 1A2. *Curr. Drug Metab.* 2009; 10:713–729. [PubMed: 19702529]
- (7). Shimada T, Gillam EM, Oda Y, Tsumura F, Sutter TR, Guengerich FP, Inoue K. Metabolism of benzo[a]pyrene to trans-7,8-dihydroxy-7, 8-dihydrobenzo[a]pyrene by recombinant human cytochrome P450 1B1 and purified liver epoxide hydrolase. *Chem. Res. Toxicol.* 1999; 12:623–629. [PubMed: 10409402]
- (8). Ueng YF, Shimada T, Yamazaki H, Guengerich FP. Oxidation of aflatoxin B1 by bacterial recombinant human cytochrome P450 enzymes. *Chem. Res. Toxicol.* 1995; 8:218–225. [PubMed: 7766804]
- (9). Van Vleet TR, Macé K, Coulombe RA. Comparative aflatoxin B(1) activation and cytotoxicity in human bronchial cells expressing cytochromes P450 1A2 and 3A4. *Cancer Res.* 2002; 62:105–112. [PubMed: 11782366]
- (10). Peterson S, Lampe JW, Bammler TK, Gross-Steinmeyer K, Eaton DL. Apiaceous vegetable constituents inhibit human cytochrome P-450 1A2 (hCYP1A2) activity and hCYP1A2-mediated mutagenicity of aflatoxin B1. *Food Chem. Toxicol.* 2006; 44:1474–1484. [PubMed: 16762476]
- (11). Wang JJ, Zheng Y, Sun L, Wang L, Yu PB, Li HL, Tian XP, Dong JH, Zhang L, Xu J, Shi W, Ma TY. CYP1A1 Ile462Val polymorphism and susceptibility to lung cancer: a meta-analysis based on 32 studies. *Eur. J. Cancer Prev.* 2011; 20:445–452. [PubMed: 22025136]
- (12). Surekha D, Sailaja K, Rao DN, Padma T, Raghunadharao D, Vishnupriya S. Association of CYP1A1\*2 polymorphisms with breast cancer risk: a case control study. *Indian J. Med. Sci.* 2009; 63:13–20. [PubMed: 19346634]
- (13). Khvostova EP, Pustyl'nyak VO, Gulyaeva LF. Genetic polymorphism of estrogen metabolizing enzymes in Siberian women with breast cancer. *Genet. Test. Mol. Biomarkers.* 2011
- (14). Chun YJ, Ryu SY, Jeong TC, Kim MY. Mechanism-based inhibition of human cytochrome P450 1A1 by rhapontigenin. *Drug Metab. Dispos.* 2001; 29:389–393. [PubMed: 11259321]
- (15). Kensler TW, Groopman JD, Sutter TR, Curphey TJ, Roebuck BD. Development of cancer chemopreventive agents: oltipraz as a paradigm. *Chem. Res. Toxicol.* 1999; 12:113–126. [PubMed: 10027787]
- (16). Gerhäuser C. Beer constituents as potential cancer chemopreventive agents. *Eur. J. Cancer.* 2005; 41:1941–1954. [PubMed: 15953717]
- (17). Foroozesh M, Primrose G, Guo Z, Bell LC, Alworth WL, Guengerich FP. Aryl acetylenes as mechanism-based inhibitors of cytochrome P450-dependent monooxygenase enzymes. *Chem. Res. Toxicol.* 1997; 10:91–102. [PubMed: 9074808]
- (18). Shimada T, Yamazaki H, Foroozesh M, Hopkins NE, Alworth WL, Guengerich FP. Selectivity of polycyclic inhibitors for human cytochrome P450s 1A1, 1A2, and 1B1. *Chem. Res. Toxicol.* 1998; 11:1048–1056. [PubMed: 9760279]
- (19). Sridhar J, Jin P, Liu J, Foroozesh M, Stevens CL. In silico studies of polyaromatic hydrocarbon inhibitors of cytochrome P450 enzymes 1A1, 1A2, 2A6, and 2B1. *Chem. Res. Toxicol.* 2010; 23:600–607. [PubMed: 20078084]



- (20). Shimada T, Tanaka K, Takenaka S, Murayama N, Martin MV, Foroozesh MK, Yamazaki H, Guengerich FP, Komori M. Structure-function relationships of inhibition of human cytochromes P450 1A1, 1A2, 1B1, 2C9, and 3A4 by 33 flavonoid derivatives. *Chem. Res. Toxicol.* 2010; 23:1921–1935. [PubMed: 21053930]
- (21). Sridhar J, Liu J, Foroozesh M, Stevens CK. Inhibition of Cytochrome P450 Enzymes by Quinones and Anthraquinones. *Chem. Res. Toxicol.* 2012; 25:357–365. [PubMed: 22185593]
- (22). Li Y, Li NY, Sellers EM. Comparison of CYP2A6 catalytic activity on coumarin 7-hydroxylation in human and monkey liver microsomes. *Eur. J. Drug Metab. Pharmacokinet.* 1997; 22:295–304. [PubMed: 9512924]
- (23). Buters JT, Schiller CD, Chou RC. A highly sensitive tool for the assay of cytochrome P450 enzyme activity in rat, dog and man. Direct fluorescence monitoring of the deethylation of 7-ethoxy-4-trifluoromethylcoumarin. *Biochem. Pharmacol.* 1993; 46:1577–1584. [PubMed: 8240414]
- (24). Born SL, Caudill D, Fliter KL, Purdon MP. Identification of the cytochromes P450 that catalyze coumarin 3,4-epoxidation and 3-hydroxylation. *Drug Metab. Dispos.* 2002; 30:483–487. [PubMed: 11950775]
- (25). Regal KA, Schrag ML, Kent UM, Wienkers LC, Hollenberg PF. Mechanism-based inactivation of cytochrome P450 2B1 by 7-ethynylcoumarin: verification of apo-P450 adduction by electrospray ion trap mass spectrometry. *Chem. Res. Toxicol.* 2000; 13:262–270. [PubMed: 10775326]
- (26). Sridar C, Kent UM, Noon K, McCall A, Alworth B, Foroozesh M, Hollenberg PF. Differential inhibition of cytochromes P450 3A4 and 3A5 by the newly synthesized coumarin derivatives 7-coumarin propargyl ether and 7-(4-trifluoromethyl)coumarin propargyl ether. *Drug Metab. Dispos.* 2008; 36:2234–2243. [PubMed: 18653744]
- (27). Chan WK, Sui Z, de Montellano P. R. Ortiz. Determinants of protein modification versus heme alkylation: inactivation of cytochrome P450 1A1 by 1-ethynylpyrene and phenylacetylene. *Chem. Res. Toxicol.* 1993; 6:38–45. [PubMed: 8448348]
- (28). Hopkins NE, Foroozesh MK, Alworth WL. Suicide inhibitors of cytochrome P450 1A1 and P450 2B1. *Biochem. Pharmacol.* 1992; 44:787–796. [PubMed: 1510726]
- (29). Burke MD, Thompson S, Weaver RJ, Wolf CR, Mayer RT. Cytochrome P450 specificities of alkoxyresorufin O-dealkylation in human and rat liver. *Biochem. Pharmacol.* 1994; 48:923–936. [PubMed: 8093105]
- (30). Shimada T, Murajama N, Tanaka K, Takenaka S, Imai Y, Hopkins NE, Foroozesh MK, Alworth WL, Yamazaki H, Guengerich FP, Komori M. Interaction of polycyclic aromatic hydrocarbons with human cytochrome P450 1B1 in inhibiting catalytic activity. *Chem. Res. Toxicol.* 2008; 21:2313–2323. [PubMed: 19548353]
- (31). Shimada T, Murayama N, Tanaka K, Takenaka S, Guengerich FP, Yamazaki H, Komori M. Spectral modification and catalytic inhibition of human cytochromes P450 1A1, 1A2, 1B1, 2A6, and 2A13 by four chemopreventive organoselenium compounds. *Chem. Res. Toxicol.* 2011; 24:1327–1337. [PubMed: 21732699]
- (32). Wu J, Cui G, Zhao M, Cui C, Peng S. Novel N-(3-carboxyl-9-benzyl-carboline-1-yl)ethylamino acids: synthesis, anti-proliferation activity and two-step-course of intercalation with calf thymus DNA. *Mol. Biosyst.* 2007; 3:855–861. [PubMed: 18000563]
- (33). Sansen S, Yano JK, Reynald RL, Schoch GA, Griffin KJ, Stout CD, Johnson EF. Adaptations for the oxidation of polycyclic aromatic hydrocarbons exhibited by the structure of human P450 1A2. *J. Biol. Chem.* 2007; 282:14348–14355. [PubMed: 17311915]
- (34). Venkatachalam CM, Jiang X, Oldfield T, Waldman M. LigandFit: a novel method for the shape-directed rapid docking of ligands to protein active sites. *J. Mol. Graph. Model.* 2003; 21:289–307. [PubMed: 12479928]
- (35). Sharma P, Ghoshal N. Exploration of a binding mode of benzothiazol-2-yl acetonitrile pyrimidine core based derivatives as potent c-Jun N-terminal kinase-3 inhibitors and 3D-QSAR analyses. *J. Chem. Inf. Model.* 2006; 46:1763–1774. [PubMed: 16859308]



- (36). Hu L, Chen G, Chau RM. A neural networks-based drug discovery approach and its application for designing aldose reductase inhibitors. *J. Mol. Graph. Model.* 2006; 24:244–253. [PubMed: 16226911]
- (37). Shrestha AR, Shindo T, Ashida N, Nagamatsu T. Synthesis, biological active molecular design, and molecular docking study of novel deazaflavin-cholestane hybrid compounds. *Bioorg. Med. Chem.* 2008; 16:8685–8696. [PubMed: 18723355]
- (38). Krovat EM, Langer T. Impact of scoring functions on enrichment in docking-based virtual screening: an application study on renin inhibitors. *J. Chem. Inf. Comput. Sci.* 2004; 44:1123–1129. [PubMed: 15154781]
- (39). Sakkiath S, Thangapandian S, John S, Kwon YJ, Lee KW. 3D QSAR pharmacophore based virtual screening and molecular docking for identification of potential HSP90 inhibitors. *Eur. J. Med. Chem.* 2010; 45:2132–2140. [PubMed: 20206418]
- (40). Sinnokrot MO, Sherrill CD. High-accuracy quantum mechanical studies of pi-pi interactions in benzene dimers. *J. Phys. Chem. A.* 2006; 110:10656–10668. [PubMed: 16970354]
- (41). Hunter CA, Singh J, Thornton JM. Pi-pi interactions: the geometry and energetics of phenylalanine-phenylalanine interactions in proteins. *J. Mol. Biol.* 1991; 218:837–846. [PubMed: 2023252]
- (42). Zhu N, Lightsey D, Liu J, Foroozesh M, Morgan KM, Stevens ED, Stevens C. L. Klein. Ethynyl and propynylpyrene inhibitors of cytochrome P450. *J. Chem. Crystallogr.* 2010; 40:343–352. [PubMed: 20473363]
- (43). Androutsopoulos VP, Papakyriakou A, Vourloumis D, Spandidos DA. Comparative CYP1A1 and CYP1B1 substrate and inhibitor profile of dietary flavonoids. *Bioorg. Med. Chem.* 2011; 19:2842–2849. [PubMed: 21482471]
- (44). Yamazaki K, Suzuki M, Itoh T, Yamamoto K, Kanemitsu M, Matsumura C, Nakano T, Sakaki T, Fukami Y, Imaishi H, Inui H. Structural basis of species differences between human and experimental animal CYP1A1s in metabolism of 3,3',4,4',5-pentachlorobiphenyl. *J. Biochem.* 2011; 149:487–494. [PubMed: 21258071]
- (45). Rosales-Hernández MC, Mendieta-Wejebe JE, Trujillo-Ferrara JG, Correa-Basurto J. Homology modeling and molecular dynamics of CYP1A1 and CYP2B1 to explore the metabolism of aryl derivatives by docking and experimental assays. *Eur. J. Med. Chem.* 2010; 45:4845–4855. [PubMed: 20813430]
- (46). Liu J, Ericksen SS, Besspiata D, Fisher CW, Szklarz GD. Characterization of substrate binding to cytochrome P450 1A1 using molecular modeling and kinetic analyses: case of residue 382. *Drug Metab. Dispos.* 2003; 31:412–420. [PubMed: 12642467]
- (47). Itoh T, Takemura H, Shimoi K, Yamamoto K. A 3D model of CYP1B1 explains the dominant 4-hydroxylation of estradiol. *J. Chem. Inf. Model.* 2010; 50:1173–1178. [PubMed: 20462226]
- (48). Lewis BC, Mackenzie PI, Miners JO. Application of homology modeling to generate CYP1A1 mutants with enhanced activation of the cancer chemotherapeutic prodrug dacarbazine. *Mol. Pharmacol.* 2011; 80:879–888. [PubMed: 21816953]

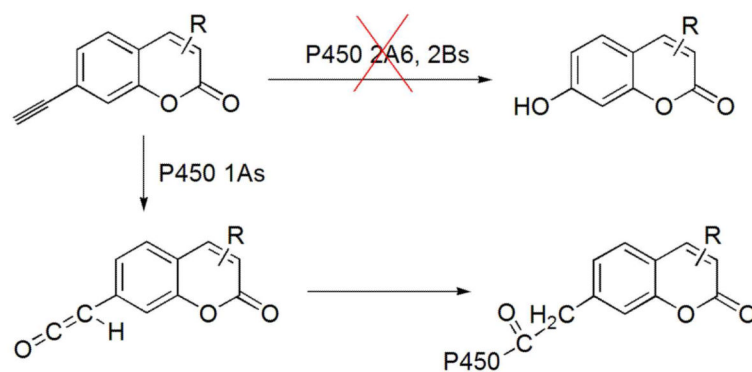


**Figure 1.** Design of 7-ethynylcoumarins as selective mechanism-based inhibitors of P450s from the 1A subfamily. The rationale for the inhibition mechanism was based on the previous investigation of aromatic acetylenes.<sup>25-27</sup>

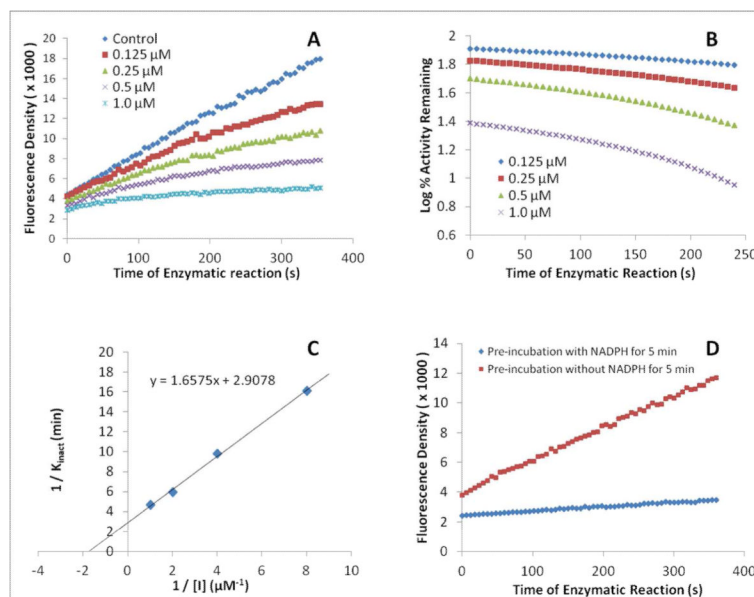


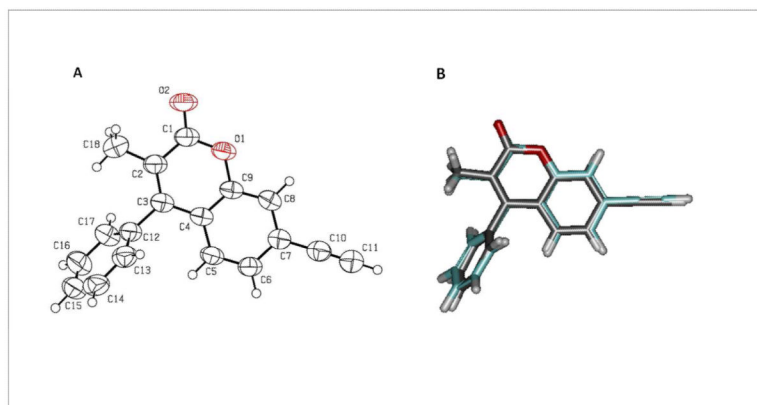
**Figure 2.**

(A) The production of resorufin by P450 1A1 in the absence (control) and presence of 0.125, 0.25, 0.5 and 1.0  $\mu\text{M}$  of 7ETMC (final concentrations). The reactions were performed at 37°C, and the formation of resorufin anion was monitored continuously over 6-min as described in the Experimental Section. Compound 7ETMC inhibits the production of resorufin in a concentration-dependent manner, and the second-order product formation curves ( $y = ax^2 + bx + c$ ) were obtained employing the Trendline tool in Microsoft Excel Program. The differential curves ( $y = 2ax + b$ ) of the product formation curves represent the instantaneous enzymatic activity values.

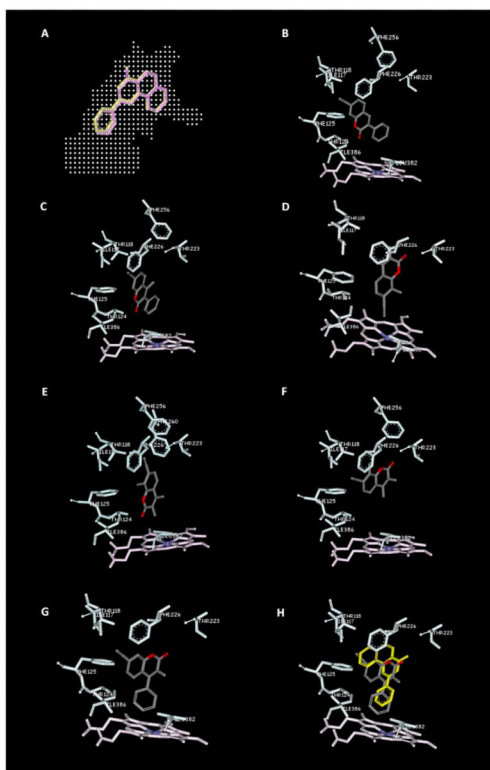
(B) Time- and concentration-dependent inhibition of P450 1A1-dependent EROD activity by compound 7ETMC. The final concentrations of 7ETMC were 0.125, 0.25, 0.5 and 1.0  $\mu\text{M}$ . The enzymatic activity values were calculated through the first-order derivatives of the product formation curves at different times, and the percentages of activity remaining was obtained according to the formula  $(A_{\text{inhibitor}}/A_{\text{control}})\%$ . The activity loss with time indicates the time-dependent inhibition of P450 1A1 by compound 7ETMC.

(C) Kitz-Wilson plots ( $1/k_{\text{inact}}$  vs.  $1/[I]$ ).  $K_{\text{inact}}$  values were obtained using the curves in graph (B) as described in the Experimental Section, and  $[I]$ s were the final concentrations of the inhibitor. In this case, the final concentrations of the inhibitor (7ETMC) were 0.125, 0.25, 0.5 and 1.0  $\mu\text{M}$ . Using the linear equation shown in this graph,  $K_I$  and limiting  $K_{\text{inact}}$  values were determined.

(D) The production of resorufin by P450 1A1 in the presence of 7ETMC (0.125  $\mu\text{M}$ ). The reaction solution underwent a 5-min pre-incubation process in the presence and absence of NADPH. The sharp decrease of product formation in the test with NADPH pre-incubation indicated that compound 7ETMC inhibited the O-deethylation activity of P450 1A1 in a NADPH-dependent manner.

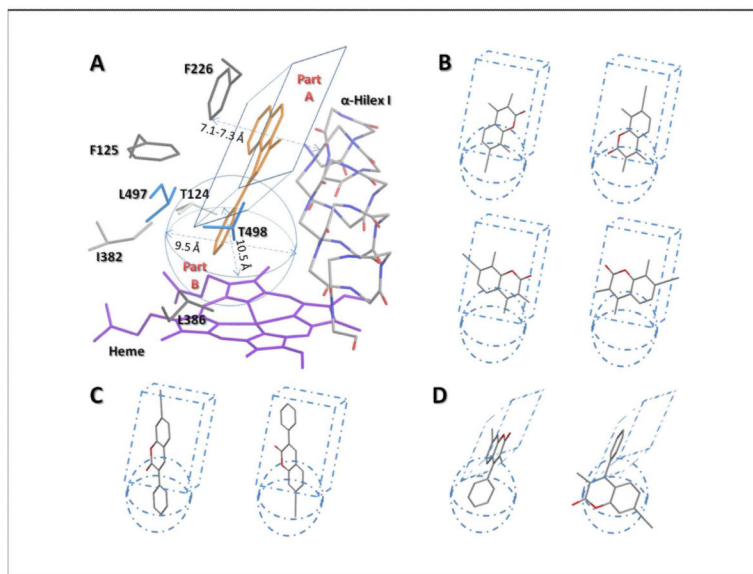
**Figure 3.**

(A) The single crystal structure of 7E3M4PC with thermal ellipsoids plotted at the 50% probability level. Due to hindrance on both sides, the 3-phenyl ring of 7E3M4PC forms a 68.8(2)° torsion angle with the plane of the coumarin core. (B) The alignment of the single crystal conformation (grey) and the computer generated minimum-energy conformation (blue) of 7E3M4PC.



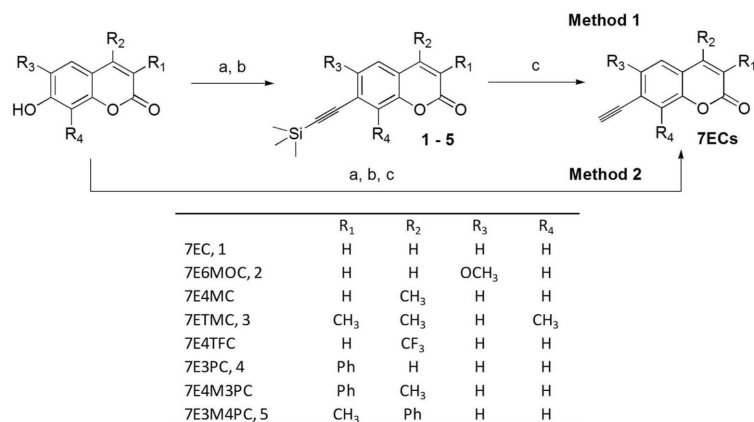
**Figure 4.**

Results and stereoviews of the docking studies. (A) Redocking of  $\alpha$ -naphthoflavone into the active site cavity of P450 1A2, yielding an RMSD value of 0.26 Å between the starting X-ray conformation of  $\alpha$ -naphthoflavone (pink) and the docked pose (yellow) suggesting a good performance of docking simulation. (B-H) The docking images of 7E3PC (B), 7E4M3PC (C), 7E3M4PC (D-F), 7E3M4PC (G), and the overlapped structures of 7E3M4PC and  $\alpha$ -naphthoflavone (yellow) (H). The heme residue is located on the bottom, and some amino acid residues (Phe-226, Phe-125, Thr-124, Leu-386, Ile-382, etc) are shown in the docking images.

**Figure 5.**

(A) The diagram of the active site cavity of P450 1A2: a narrow, but extended channel (Part A), and a spherical hydrophobic pocket (Part B). (B) The binding patterns of compound 7ETMC with P450 1A2, which suggests that the mid-size 7-ethynylcoumarins could freely rotate in the narrow cavity (Part A) if only it is parallel with Phe-226 and the peptide bond in the  $\alpha$ -helix I in order to form  $\pi$ - $\pi$  interactions. (C) The possible binding patterns of compound 7E3PC with P450 1A2. Phenyl-facing-heme orientation (left) takes an obvious priority over the acetylene-facing-heme orientation (right). (D) The possible binding pattern (left) and impossible binding pattern (right) of compound 7E3M4PC with P450 1A2, suggesting that there is no reactive pose for the docking of 7E3M4PC with this enzyme.

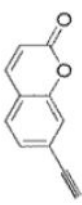
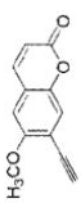
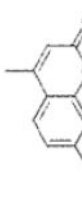
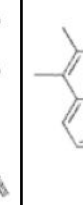
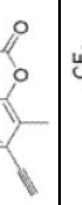
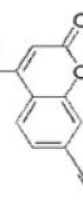
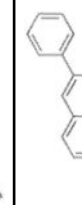


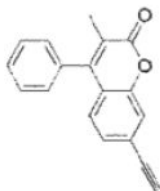
**Scheme 1.**

The synthetic route of 7-ethynylcoumarins. Reagents and conditions: a) Triflic anhydride, pyridine, 0 °C, 2 h; b) Pd(PPh<sub>3</sub>)<sub>2</sub>Cl<sub>2</sub>, copper(I) iodide, trimethylsilylacetylene, diisopropylamine, reflux, 2 h; c) tetrabutylammonium fluoride, methanol, 70 °C, 0.5 h.

**Table 1**

Inhibition activities of 7ECs on P450s 1A1, 1A2, 2A6, and 2B1 represented as IC<sub>50</sub> values (Calculations are based on the first 6 min of the enzymatic reaction).

Enzyme	ID	1A1	1A2	2A6	2B1
		IC <sub>50</sub> value (μM)			
	7EC	>50	15.8	>50	>50
	7E6MOC	48.5	48.3	>50	>50
	7E4MC	10.8	2.20	>50	>50
	7ETMC	0.50	0.46	>50	>50
	7E4TFC	14.3	2.69	>50	15.1
	7E3PC	0.63	3.00	>50	>50
	7E4M3PC	4.48	5.80	>50	>50

Enzyme	ID	1A1	1A2	2A6	2B1
		IC <sub>50</sub> value (μM)			
Structure		2.93	1.68	>50	9.16

**Table 2**The  $K_I$ , limiting  $K_{inact}$  and  $K_a$  values of the inhibitors on P450 1A1

Compound	$K_I$ ( $\mu\text{M}$ )	limiting $K_{inact}$ ( $\text{min}^{-1}$ )	$K_a$ ( $\mu\text{M}$ )
7EC	ND	ND	ND
7E6MOC	104.03	0.34	0.11
7E4MC	38.60	0.21	0.25
7ETMC	0.57	0.34	1.23
7E4TFC	16.85	0.23	0.29
7E3PC	0.38	0.25	0.93
7E4M3PC	5.16	0.31	0.33
7E3M4PC	3.58	0.37	0.38

ND: Not Determined

**Table 3**The  $K_I$ , limiting  $K_{inact}$ , and consensus scores of the inhibitors on P450 1A2

Compound	$K_I$ ( $\mu\text{M}$ )	limiting $K_{inact}$ ( $\text{min}^{-1}$ )	Consensus score
7EC	5.83	0.09	0
7E6MOC	78.90	0.35	2
7E4MC	2.65	0.39	3
7ETMC	0.87	0.44	3
7E4TFC	3.15	0.31	3
7E3PC	0.65	0.03	5
7E4M3PC	0.83	0.10	4
7E3M4PC	ND	ND	2

ND: Not Determined